Bayesian Methods in the Study of Detection Thresholds in Visuo-Haptic Illusions

Nargiz Askarbekkyzy

Abstract

Large-scale haptic displays have the potential to create fully immersive experiences in Virtual Reality (VR). Floor-based pin-array displays can simulate complex terrains and environments. When combined with two visuo-haptic illusions—angle redirection and scaling-up—these displays can further enhance the immersion. In our previous work, we determined the detection threshold for the stimuli (angle and scale) distortion beyond which the user could detect the visuo-haptic illusion for floor shape displays, thereby breaking the "realness" of the VR experience. In this paper, we revisit the visuo-haptic illusions, employing Bayesian methods to estimate the detection thresholds more precisely by incorporating prior knowledge.

1 Introduction

1.1 Haptic displays

Incorporating haptic feedback into navigation within virtual environments enhances realistic immersion and walking experiences [7]. One approach to delivering haptic feedback is through haptic floors. These floors use built-in actuators to provide tactile sensations to the users' feet, imitating the physical properties of ground materials [13], the crinkling of fragile structures [8], assisting with navigation and direction [4], and more.

Haptic shape displays render virtual objects that users can perceive and interact with through touch. Prominent examples include TilePoP [12] and LiftTiles [11], which are 2D arrays of inflatable actuators used for prototyping room-scale objects such as furniture and cars. However, a significant drawback of these shape displays is their low resolution. Each tile measures 30 cm $\times$ 30 cm, which limits the range of objects in VR that could be rendered in the real world. The issue of low resolution was addressed by Elevate [5]. The authors introduced a 1.80 $\times$ 0.60 m platform consisting of 3 cm $\times$ 3 cm pins, allowing for more fine-grained rendering. Though it also has its limitation. Elevate is not scalable enough and building a bigger platform will require higher costs and more complex system. To tackle these issues, the usage of visuo-haptic illusions was suggested. They could effectively overcome the physical scalability and resolution limitations by leveraging perceptual tricks without higher hardware specifications.

1.2 Visuo-haptic illusion

The visual dominance effect, where the visual shape overrides the perceived tactile shape of the object [10], is often employed in VR applications. Combined with pseudo-haptic feedback, visual cues can modify the perceived material, texture, stiffness [6], or shape of a proxy object [3], even if it is physically different from the virtual object it represents. This allows seamless interactions in VR, despite the disparity between physical and virtual forms.

Applying visuo-haptic illusions to improve the perceived resolution and performance of the tabletop shape displays was suggested by Abtahi and Follmer [1]. They employed retargeting technique and redirection of the virtual hand placement to create an illusion of moving along a sloped line while physically moving the hand along a horizontal line (angle redirection). They also mapped smaller physical objects onto larger virtual object by manipulating the virtual output displacement relative to the physical displacement of the input device (scaling-up). Moreover, they manipulated the perceived speed of the pins during the shape render.

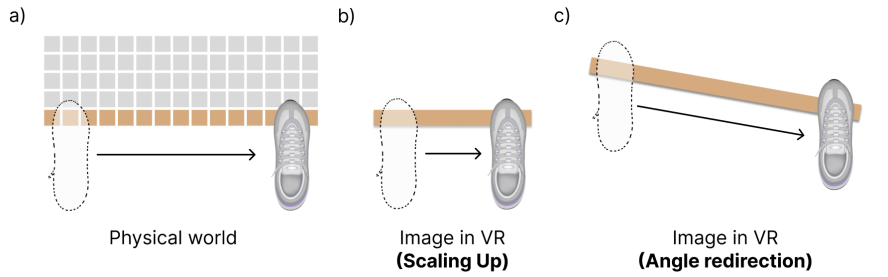

Figure 1: a) The user moves their foot from left to right along the shape display. (b) When the scaling-up technique is applied, the virtual foot's displacement is scaled down. (c) When the angle redirection technique is applied, the virtual foot is redirected.

In my previous contribution, I adapted the methodology introduced by Abtahi and Follmer to apply visuo-haptic illusions on the floor-based shape displays [2]. Due to the differences in the available hardware, only the angle redirection and scaling up techniques were explored. The visual explanation of the techniques is presented in the Figure 1.

The study consisted of two parts. In the first part, we determined the detection threshold for visuo-haptic illusion techniques. Here, the detection threshold is the minimum value of the stimulus (angle or scale) distortion at which the user can clearly detect the presence of visuo-haptic illusion [9]. It means that if the stimulus intensity is lower than the detection threshold, an individual does not experience disparity between what they see and what they feel.

In the second part, after we found the extent to which we can distort angles and scales without detection, we explored the effectiveness of visuo-haptic illusions in actually improving the resolution and smoothness of the shape display.

In this report, we revisit the first part of the previous study, specifically the identification of detection thresholds. This time, we adopt a Bayesian approach to analyze the results, offering a probabilistic estimation of the thresholds.

2 Data

In this project, we use the data collected in the previous work using the method of constant stimuli [2]. The two main stimulus types explored were angle and scale. Each stimulus distortion was tested in two conditions: barefoot and shod (with shoes on). In total, there were 4 subparts exploring each combination: angle redirection with barefoot condition, angle redirection with shod condition, scaling up with barefoot condition, and scaling up with shod condition.

In each subpart, users were presented with multiple levels of stimulus distortion. For angle redirection, we tested 13 different angles: from 5° to 65° in 5° intervals. For scaling up, we tested five different scale factors: 1x, 1.14x, 1.33x, 1.6x, and 2x. Each stimulus intensity was presented to the user four times within each subpart. Thus, each user went through 52 samples for angle redirection and 20 samples for scaling up in a subpart.

After each sample, users were asked whether they detected the illusion, responding with "yes" or "no," and then rated their confidence in the answer on a scale from 1 to 5.

The detection ratio for each participant in the study was calculated for each stimulus in each subpart. The illusion was counted as detected if the participant's confidence level was at least 3. The count of the detection of the stimulus sample was divided by total number of trials with this stimulus sample, which is 4, to find the detection ratio.

There were 16 participants in this part of the study, so in the end, we had four datasets: two for angle redirection and two for scaling up. The datasets are organized as follows:

- Each row corresponds to a participant, denoted as P_i, where $i = 1, 2, \ldots, 16$.
- Each column corresponds to a distortion intensity, represented in degrees for angle redirection and scales for scaling up.

The dataset matrices are given in Table 1 and Table 2.

Participant ID	5°	10°	15°	20°	25°	30°	⋯	65°
P_1	value	value	value	value	value	value	⋯	value
P_2	value	value	value	value	value	value	⋯	value
⋮	⋮	⋮	⋮	⋮	⋮	⋮	⋯	⋮
P_n	value	value	value	value	value	value	⋯	value

Table 1: Dataset matrix where each row represents a participant and each column represents a distortion intensity from 5° to 65°.

Participant ID	1×	1.14×	1.33×	1.6×	2×
P_1	value	value	value	value	value
P_2	value	value	value	value	value
⋮	⋮	⋮	⋮	⋮	⋮
P_n	value	value	value	value	value

Table 2: Dataset matrix where each row represents a participant and each column represents a scaling factor $(1\times, 1.14\times, 1.33\times, 1.6\times, 2\times)$.

3 Methodology

To determine the detection thresholds, the data is fitted to a psychometric function of sigmoid shape, which represents the response of the observer to the change in the stimulus intensity. The detection threshold is chosen as a stimulus intensity at which the detection probability is 75%, following the previous literature [1, 2].

In this project, we first replicate the original findings of the previous work made in MATLAB using Python. After that we apply various Bayesian approaches to fit a psychometric function.

Moreover, we previously used Wilcoxon signed-rank test to find if having shoes on has a significant impact on the illusion perception. In this project, we use one-way ANOVA to determine it.

3.1 Frequentist approach

The previous work used the frequentist approach. The psychometric function was modeled using logistic regression, relating the probability of detection (P) as a function of the stimulus intensity (x) with the following form:

$$P(x) = \frac{1}{1 + \exp(-(\beta_0 + \beta_1 x))}$$

where β_1 is the slope parameter, and β_0 is the threshold parameter.

To estimate these parameters, we apply maximum likelihood estimation (MLE). The likelihood function for logistic regression can be written as:

$$L(\beta_0, \beta_1) = \prod_{i=1}^{n} \left[P(x_i)^{y_i}(1 - P(x_i))^{1-y_i}\right]$$

where y_i represents the binary response (0 or 1) for each trial, and x_i is the stimulus intensity presented in the i-th trial. Then we take log-likelihood

$$l(\beta_0, \beta_1) = \sum_{i=1}^{n} y_i log(P(x_i)) + (1 - y_i) log(1 - P(x_i))$$

The parameters b and c are chosen to maximize the log-likelihood. We use statsmodels Python package for estimation.

3.2 Bayesian approach

In the Bayesian approach, we model the parameters of the psychometric function probabilistically by incorporating prior knowledge into the estimation. We use the same likelihood function as in the frequentist approach, but now also defining a prior distribution for the parameters.

To apply the Bayesian method, we first transform the data so that it contains two columns: one for the stimulus intensity (x) and one for the binary detection outcome (y). Here $y = 1$ indicates detection of the illusion with confidence in the answer ≥ 3, and $y = 0$ indicates either no detection or detection with low confidence in the answer. This transformation allows us to apply Bayesian inference to estimate the parameters of the psychometric function.

3.2.1 Logistic regression

For the Bayesian logistic regression model, we use logit link function:

$$\log(\frac{p}{1-p}) = \beta_0 + \beta_1 x$$

The model is as follows:

$$\begin{aligned} y_i &\sim Bern(p) \\ p &= \text{invlogit}(\beta_0 + \beta_1 x) \\ \beta_0 &\sim N(0, \sigma_0^2 = 10^2) \\ \beta_1 &\sim N(0, \sigma_1^2 = 10^2) \end{aligned}$$

We use PyMC to run the simulation, sample from the posterior and estimate the parameters.

3.2.2 Logistic regression with random effects

Individual participants might introduce randomness, which we might need to account for. To model this, we introduce random effects to the intercepts for each participant. The logistic regression model with random effects:

$$\begin{aligned} y_{ij} &\sim Bern(p) \\ p &= \text{invlogit}(\beta_0 + \beta_1 x_i j + u_j) \\ \beta_0 &\sim N(0, \sigma_0^2 = 10^2) \\ \beta_1 &\sim N(0, \sigma_1^2 = 10^2) \\ \tau &\sim Gamma(0.01, 0.01) \\ u_j &\sim N(0, \sigma_1^2 = (1/\tau)^2) \end{aligned}$$

We use PyMC to run the simulation, sample from the posterior and estimate the parameters.

3.2.3 Wichmann and Hall method

An alternative method for fitting psychometric functions is the Wichmann and Hall method. It introduces a guess rate γ and a lapse rate λ [14]:

$$\begin{aligned} P(x; \beta_0, \beta_1, \gamma, \lambda) &= \gamma + (1 - \gamma - \lambda) F(x; \beta_0, \beta_1) \\ F(x; \beta_0, \beta_1) &= \frac{1}{1 + \exp(-(\beta_0 + \beta_1 x))} \\ \beta_0 &\sim N(0, \sigma_0^2 = 10^2) \\ \beta_1 &\sim N(0, \sigma_1^2 = 10^2) \\ \gamma &\sim Beta(2, 50) \\ \lambda &\sim Beta(2, 50) \end{aligned}$$

.

Here, the guess rate γ acts as a lower bound, while λ in this scenario is perceived as a miss rate, representing how often participants answered incorrectly. In this section, we do not put additional constraints on γ and λ besides the non-informative priors.

3.2.4 Wichmann and Hall method with constraints

[14] suggests that the guess rate is equal to a $\frac{1}{n}$, where n is number of alternative forced choices. In yes/no scenarios, $\gamma = 0.5$. The literature also suggests that usually the λ is set to 0, which is same as Bayesian Logistic regression. However, it does not account for lapses well, so it is recommended to put a narrow constraint of [0, 0.06] on λ. Our model in this case is:

$$
\begin{aligned}
P(x; \beta_0, \beta_1, \gamma, \lambda) &= \gamma + (1 - \gamma - \lambda) F(x; \beta_0, \beta_1) \\
F(x; \beta_0, \beta_1) &= \frac{1}{1 + \exp(-(\beta_0 + \beta_1 x))} \\
\beta_0 &\sim N(0, \sigma_0^2 = 10^2) \\
\beta_1 &\sim N(0, \sigma_1^2 = 10^2) \\
\gamma &= 0.5 \\
\lambda &\sim Beta(2, 50) * 0.06
\end{aligned}
$$

3.2.5 Analysis of variance

Finally, we assess the effects of different experimental conditions: barefoot vs. shod. We perform an analysis of variance (ANOVA) on the detection threshold estimates for each stimulus intensity across conditions. This allows us to find whether the footwear condition has an impact.

The ANOVA model is expressed as:

$y_{ij} \sim N(\mu_{ij}, \sigma^2)$	likelihood
$\mu_j \sim N(0, \sigma_0^2)$	prior: grand mean for stimulus intensity j
$\mu_{ij} = \mu_j + a_{ij}$	deterministic relationship
$a_{ij} \sim N(0, \sigma_i^2)$	prior: $a_{ij} \quad i = 1, 2$ for conditions
$\tau \sim Ga(0.001, 0.001)$	prior: τ
$\sigma^2 = 1/\tau$	deterministic relationship
Subject to: $a_{1j} + a_{2j} = 0$	STZ constraint

where y_{ij} represents the detection threshold for the i-th condition, j-th stimulus intensity, μ_j is the overall mean for j-th stimulus intensity, α_{ij} represents the effect of the i-th experimental condition, j-th stimulus intensity.

The significance of the effects is tested by analyzing the means of $\alpha_{1j} - \alpha_{2j}$ and the credible sets for them. If all $\alpha_{1j} - \alpha_{2j}$ contain 0 in their credible set, then the footwear condition does not have effect on the illusion.

4 Results

We present the results of parameter estimations using various approaches, along with the pcyshometric function fits and the corresponding detection threshold in this section. The plots show average detection ratios as a function of stimulus distortion. The error bars in the plots refer to the standard error. The detection thresholds correspond to the stimulus intensity that yields 75% detection probability. Table 3 summarizes the detection thresholds.

Function	Angle, barefoot	Angle, shod	Scale, barefoot	Scale, shod
Frequentist logistic regression	42.82°	45.37°	1.55x	1.58x
Bayesian logistic regression	42.79°	45.31°	1.55x	1.58x
Bayesian logistic regression with random effects	38.21°	38.65°	1.49x	1.53x
Bayesian logistic regression with guess and lapse rate	42.22°	45.1°	1.55x	1.58x
Bayesian logistic regression with constrained guess and lapse rate	45.22°	47.92°	1.66x	1.67x

Table 3: Parameter estimations using Bayesian logistic regression

Stimulus	Condition	β_0 mean	β_0 95%	β_1 mean	β_1 95%
Angle	Barefoot	-2.7963	[-6.153, 0.560]	0.0910	[-0.004, 0.186]
Angle	Shod	-2.8990	[-6.295, 0.497]	0.0881	[-0.004, 0.181]
Angle	Barefoot	-8.4527	[-22.546, 5.640]	6.1485	[-4.277, 16.574]
Scale	Shod	-7.4986	[-20.209, 5.212]	5.4498	[-3.912, 14.812]

Table 4: Parameter estimations using frequentist approach

4.1 Frequentist approach

In this subsection, we used frequentist approach to estimate the parameters of the psychometric function for each condition and their 95% confidence intervals. The results are summarized in Table 4. Figures 2 and 3 show the psychometric function fits using the mean values of estimated parameters.

4.2 Bayesian approach

4.2.1 Logistic regression

The results of the Bayesian logistic regression model for each condition are summarized in Table 5. The model estimates the slope and intercept parameters, along with their 95% credible sets. Figures 4 and 5 show the psychometric function fits using the mean values of estimated parameters.

4.2.2 Logistic regression with random effects

The results of the Bayesian logistic regression model with random effects for each condition are summarized in Figure 6 and 7. The model estimates the slope and intercept parameters, along with their 95% credible sets. Figures 8 and 9 show the psychometric function fits using the mean values of estimated parameters.

4.2.3 Wichmann and Hall method

The results of the Bayesian logistic regression model with guess and lapse rates for each condition are summarized in Figure 10 and 11. The model estimates the slope and intercept parameters, along with their 95% credible sets. Figures 12 and 13 show the psychometric function fits using the mean values of estimated parameters.

Stimulus	Condition	β_0 mean	β_0 95%	β_1 mean	β_1 95%
Angle	Barefoot	-2.810	[-3.219, -2.389]	0.091	[0.080, 0.103]
Angle	Shod	-2.909	[-3.341, -2.499]	0.088	[0.077, 0.100]
Angle	Barefoot	-8.430	[-10.204, -6.826]	6.143	[4.867, 7.377]
Scale	Shod	-7.491	[-9.017, -5.901]	5.454	[4.249, 6.555]

Table 5: Parameter estimations using Bayesian logistic regression

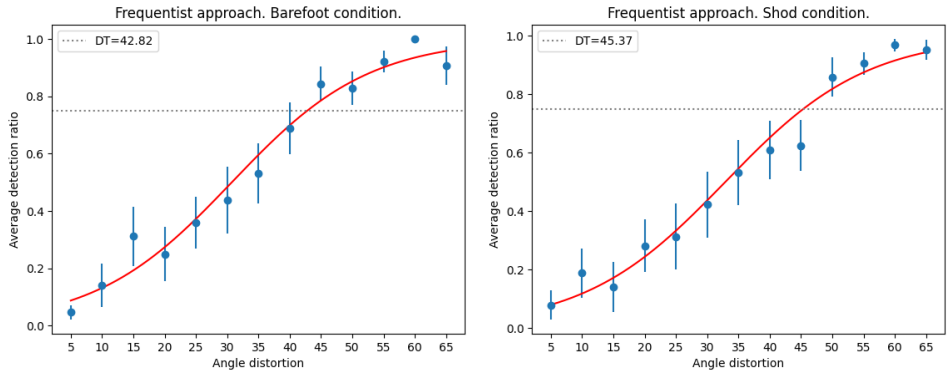

(a) Barefoot condition (b) Shod condition

Figure 2: Average detection ratio as a function of angle distortion using the frequentist approach: (a) DT is 42.82° for the barefoot condition; (b) DT is 45.37° for the shod condition.

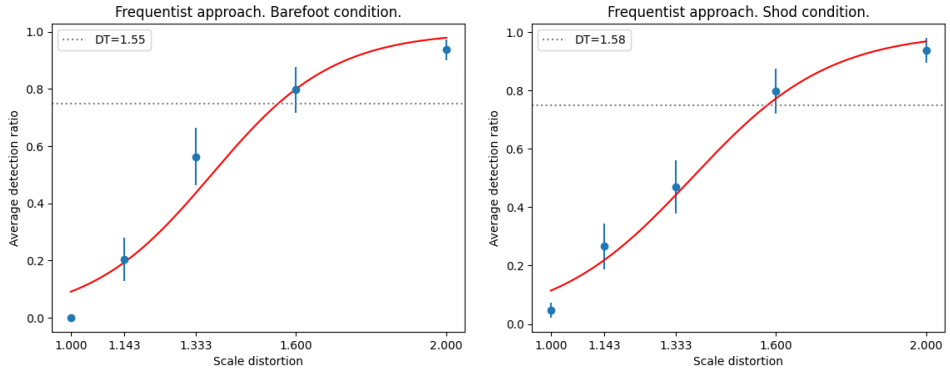

(a) Barefoot condition (b) Shod condition

Figure 3: Average detection ratio as a function of scale distortion using the frequentist approach: (a) DT is 1.55x for the barefoot condition; (b) DT is 1.58x for the shod condition.

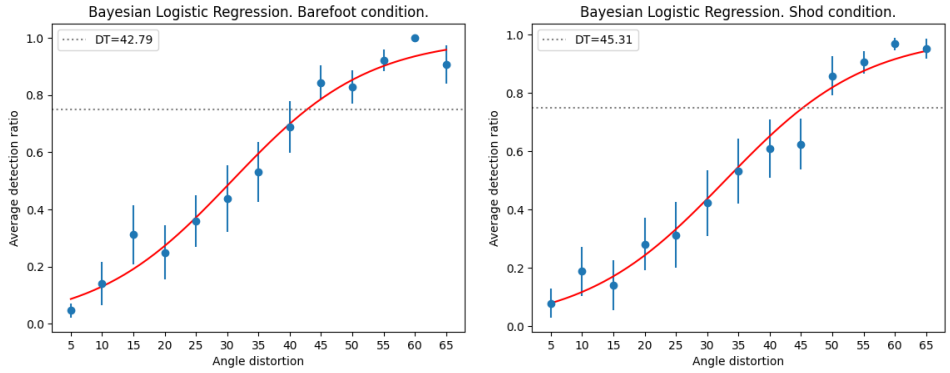

(a) Barefoot condition (b) Shod condition

Figure 4: Average detection ratio as a function of angle distortion using Bayesian logistic regression: (a) DT is 42.79° for the barefoot condition; (b) DT is 45.31° for the shod condition.

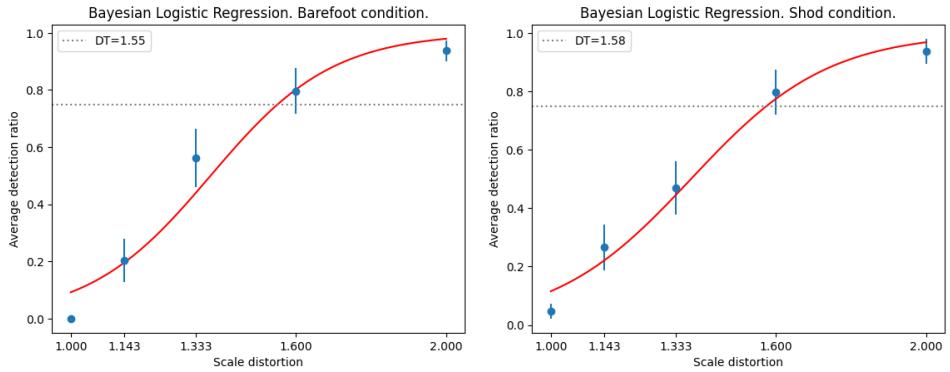

(a) Barefoot condition (b) Shod condition

Figure 5: Average detection ratio as a function of scale distortion using Bayesian logistic regression: (a) DT is 1.55x for the barefoot condition; (b) DT is 1.58x for the shod condition.

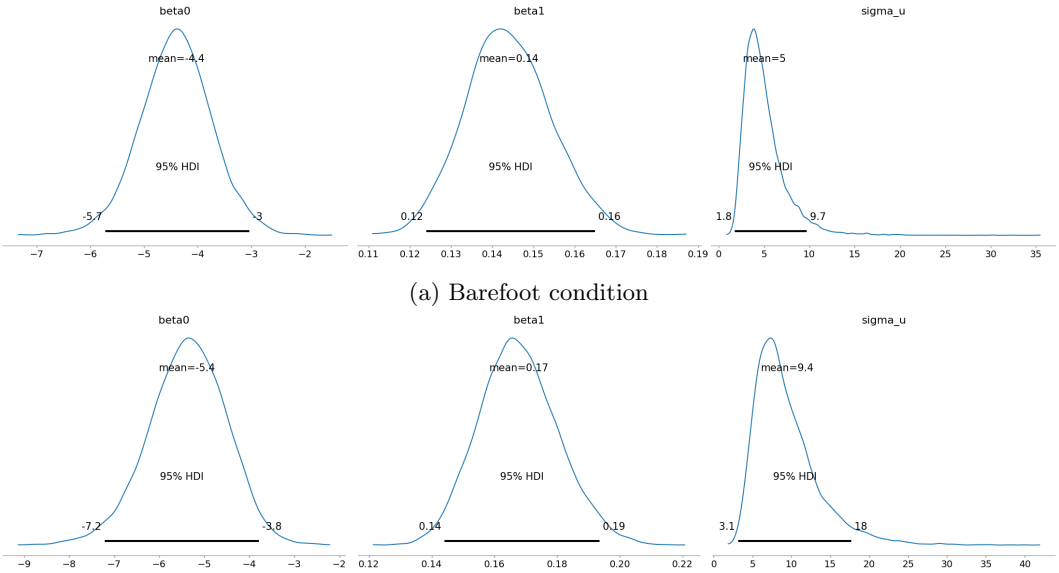

(a) Barefoot condition

(b) Shod condition

Figure 6: Posterior distribution of parameters for Bayesian logistic regression with random effects: (a) Angle redirection and barefoot condition; (b) Angle redirection and shod condition;

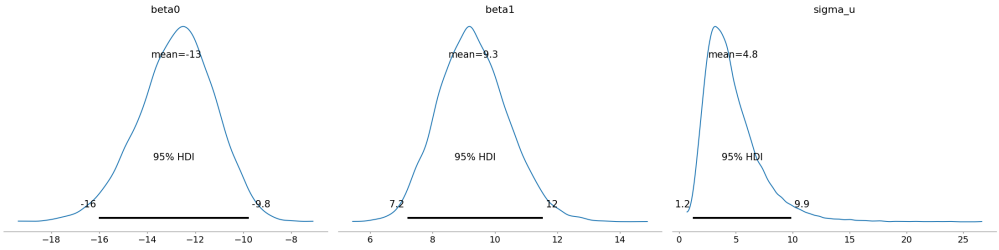

(a) Barefoot condition

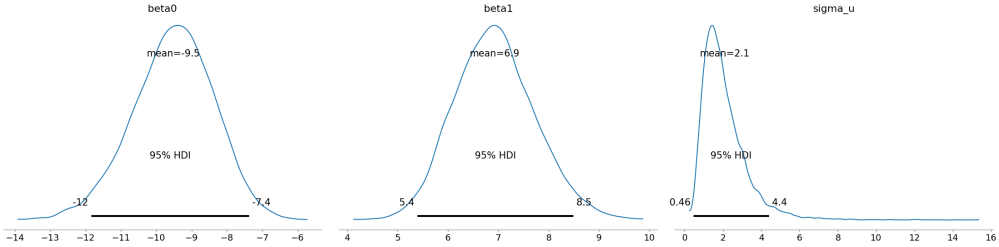

(b) Shod condition

Figure 7: Posterior distribution of parameters for Bayesian logistic regression with random effects: (a) Scaling up and barefoot condition; (b) Scaling up and shod condition;

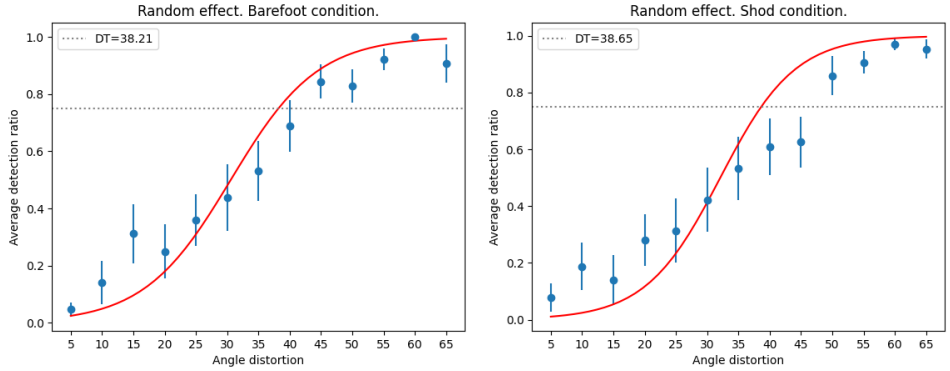

(a) Barefoot condition (b) Shod condition

Figure 8: Average detection ratio as a function of angle distortion using Bayesian logistic regression with random effects: (a) DT is 38.21° for the barefoot condition; (b) DT is 38.65° for the shod condition.

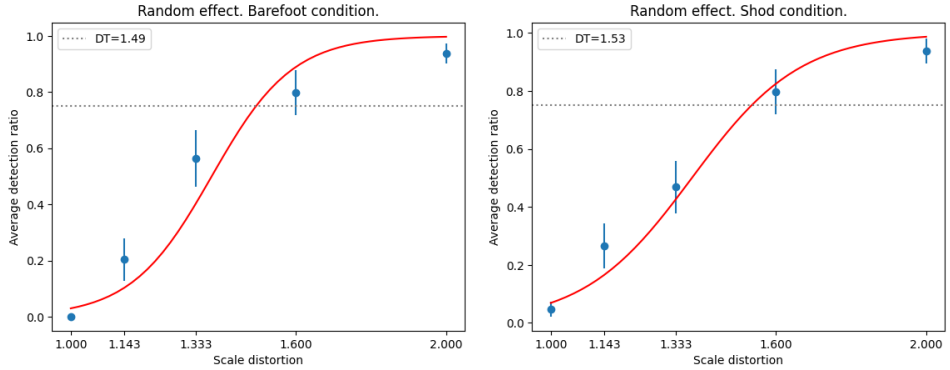

(a) Barefoot condition (b) Shod condition

Figure 9: Average detection ratio as a function of scale distortion using Bayesian logistic regression with random effects: (a) DT is 1.49x for the barefoot condition; (b) DT is 1.53x for the shod condition.

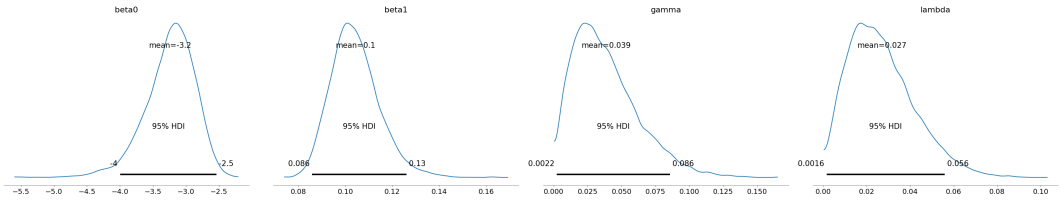

(a) Barefoot condition

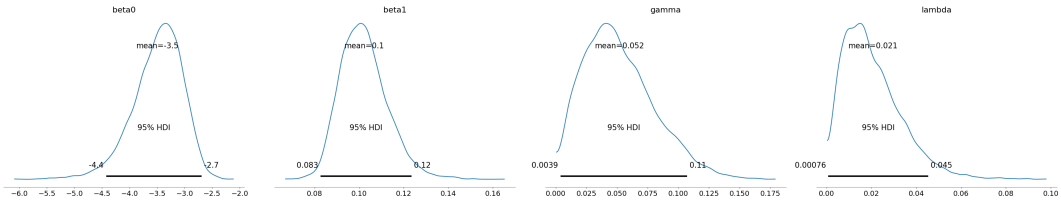

(b) Shod condition

Figure 10: Posterior distribution of parameters for Bayesian logistic regression with guess and lapse rates: (a) Angle redirection and barefoot condition; (b) Angle redirection and shod condition;

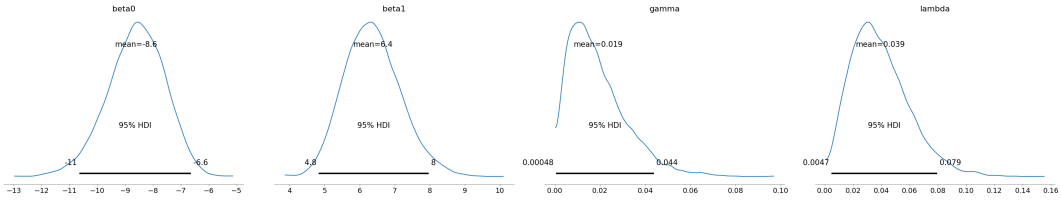

(a) Barefoot condition

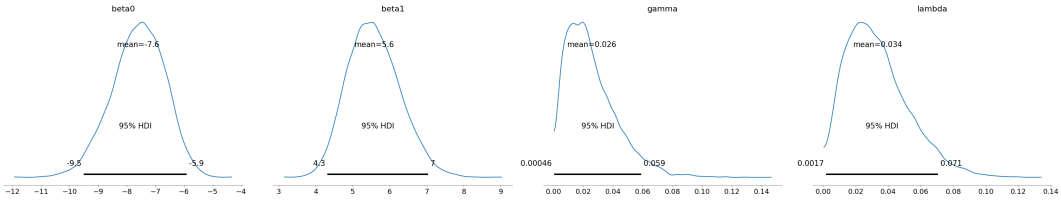

(b) Shod condition

Figure 11: Posterior distribution of parameters for Bayesian logistic regression with guess and lapse rates: (a) Scaling up and barefoot condition; (b) Scaling up and shod condition;

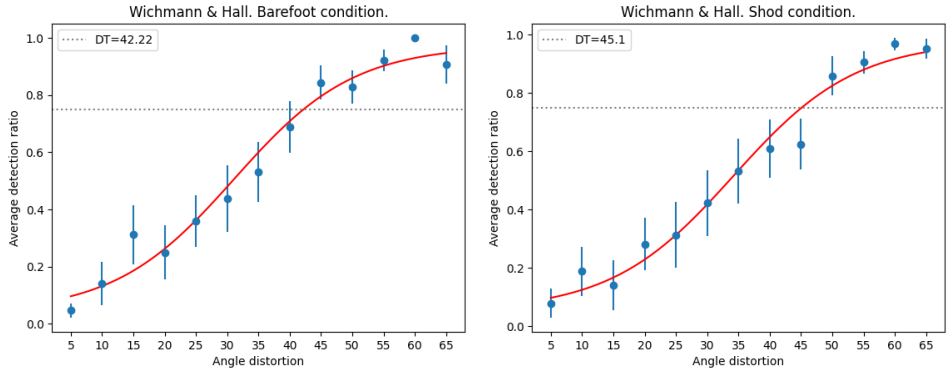

(a) Barefoot condition

(b) Shod condition

Figure 12: Average detection ratio as a function of angle distortion using Bayesian logistic regression with guess and lapse rates: (a) DT is 42.22° for the barefoot condition; (b) DT is 45.1° for the shod condition.

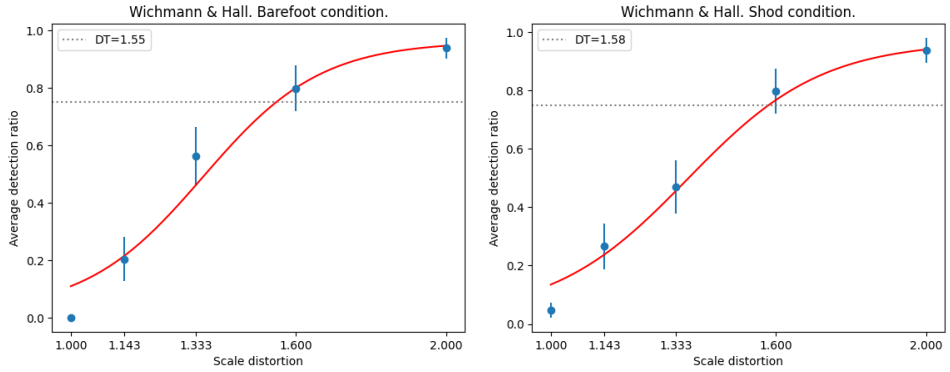

(a) Barefoot condition (b) Shod condition

Figure 13: Average detection ratio as a function of scale distortion using Bayesian logistic regression with guess and lapse rates: (a) DT is 1.55x for the barefoot condition; (b) DT is 1.58x for the shod condition.

4.2.4 Wichmann and Hall method with fixed guess rate

The results of the Bayesian logistic regression model with fixed at 0.5 guess rate and constrained lapse rate for each condition are summarized in Figure 14 and 15. The model estimates the slope and intercept parameters, along with their 95% credible sets. Figures 16 and 17 show the psychometric function fits using the mean values of estimated parameters.

4.2.5 Analysis of variance

On-way ANOVA test was performed to investigate differences in detection ratios for various stimulus intensity across two footwear conditions: barefoot vs. shod. The findings in Figure 18 suggest that there is no significant difference between two conditions as all the differences contain 0 in their credible set.

5 Discussion

Table 3 provides findings of a comparative analysis detection thresholds across different modeling approaches and footwear conditions for both angle and scale distortions.

First, frequentist logistic regression and Bayesian logistic regression yield almost identical results in terms of the posterior means of the parameters, leading to similar detection thresholds across all conditions. However, the credible sets of slope and intercept in Bayesian logistic regression are way narrower than the credible interval in the classic logistic regression, which signifies higher confidence in the mean value.

Second, we introduced random effects into the Bayesian logistic regression to account for the randomness for each study participant. It led to lower estimates for detection thresholds compared to the other methods. For instance, the angle DTs in the barefoot and shod conditions decreased to 38.21° and 38.65°, respectively. It could mean that there is significant individual variability in the perception of the visuo-haptic illusions. Some participants are more sensitive to the illusions, while some are prone to believe in them. Lower DTs mean that the visuo-haptic illusion range is lower than what was originally expected.

Third, we incorporate guess and lapse rates into the Bayesian logistic regression model. They allow to take into account the errors made by the participants in the study. When the guess and lapse rates are not constrained, the results are slightly lower than the results of frequentist and Bayesian logistic regression, indicating that there were some guesses and errors in the participant behavior.

However, as there are two alternative forced choices, participants could guess based on their intuition. In this case, the guess rate is fixed to be 0.5 and lambda is constrained to be small, yet non-zero. The guess rate serves as the lower bound. In all the previous cases, the detection ratios at lower stimuli were low. The increased lower bound also led to higher detection threshold estimates, particularly for

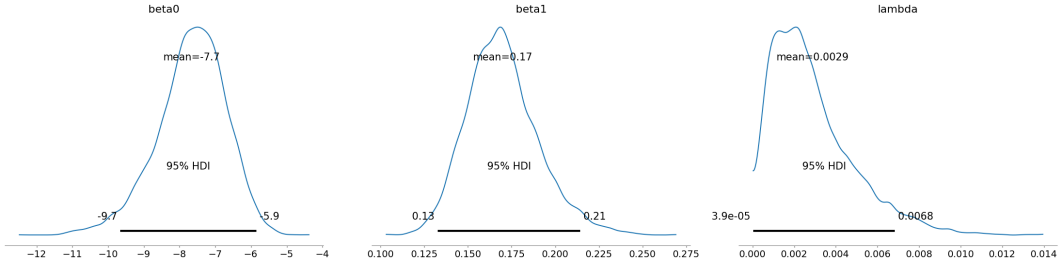

(a) Barefoot condition

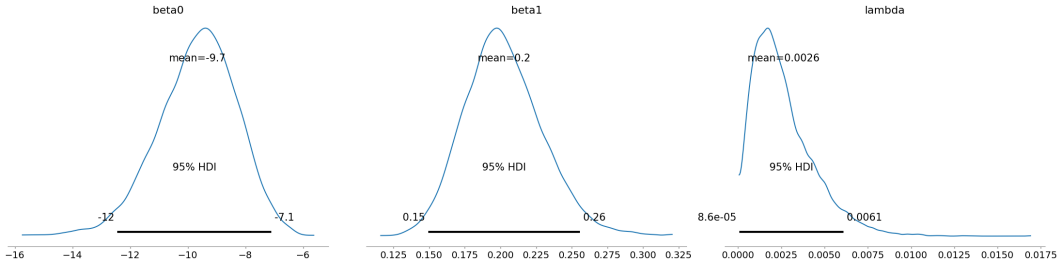

(b) Shod condition

Figure 14: Posterior distribution of parameters for Bayesian logistic regression with constrained guess and lapse rates: (a) Angle redirection and barefoot condition; (b) Angle redirection and shod condition;

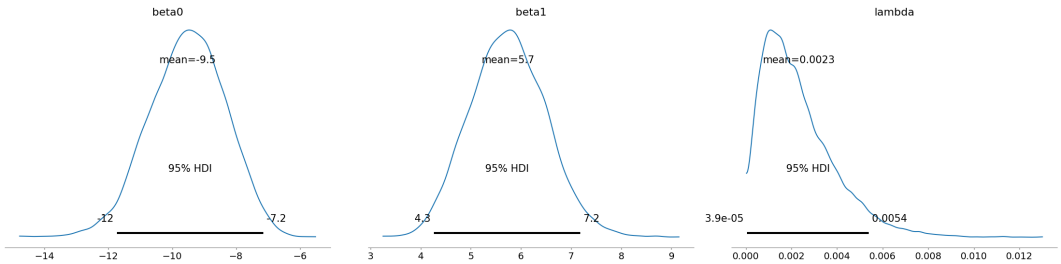

(a) Barefoot condition

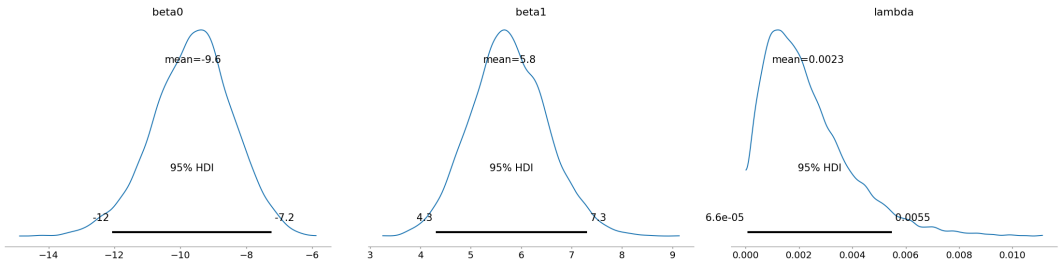

(b) Shod condition

Figure 15: Posterior distribution of parameters for Bayesian logistic regression with constrained guess and lapse rates: (a) Scaling up and barefoot condition; (b) Scaling up and shod condition;

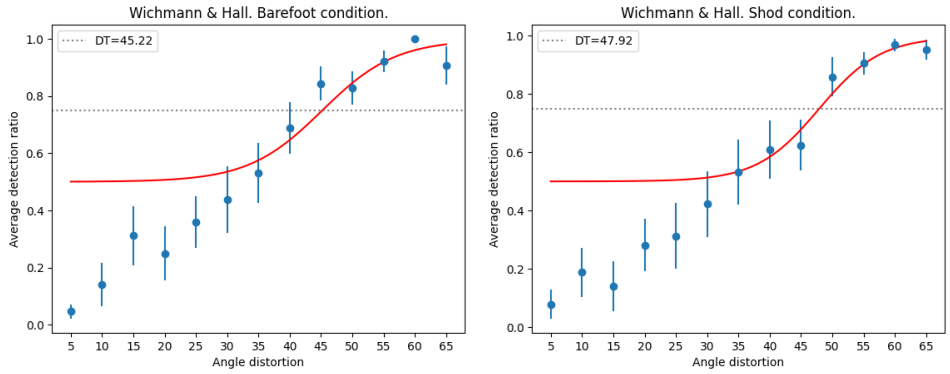

(a) Barefoot condition (b) Shod condition

Figure 16: Average detection ratio as a function of angle distortion using Bayesian logistic regression with constrained guess and lapse rates: (a) DT is 45.22° for the barefoot condition; (b) DT is 47.92° for the shod condition.

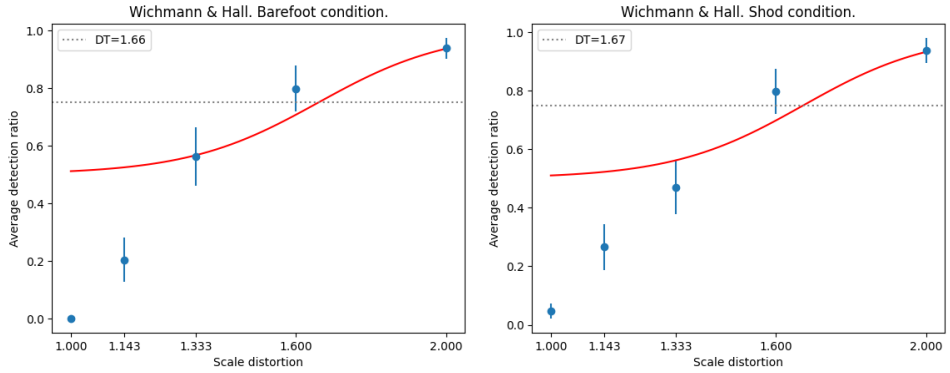

(a) Barefoot condition (b) Shod condition

Figure 17: Average detection ratio as a function of scale distortion using Bayesian logistic regression with constrained guess and lapse rates: (a) DT is 1.66x for the barefoot condition; (b) DT is 1.67x for the shod condition.

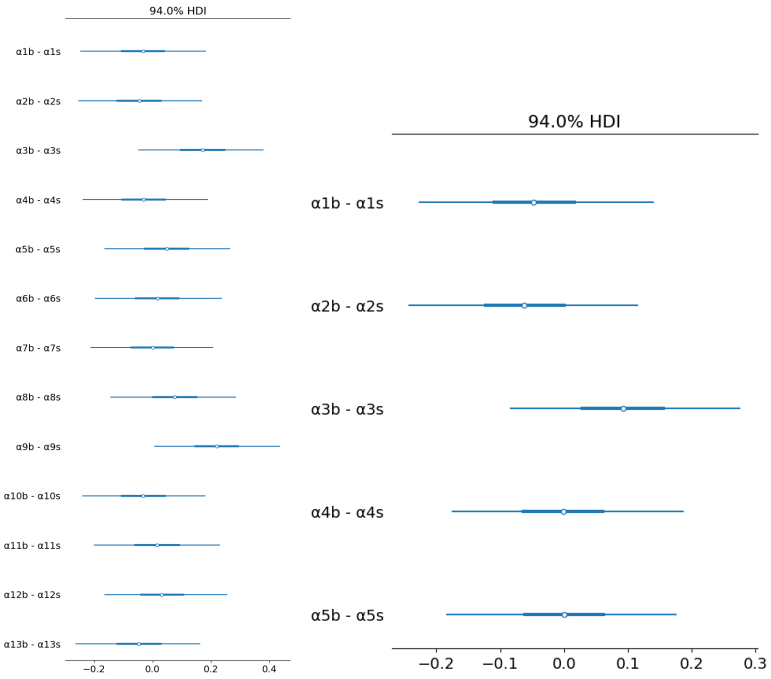

(a) Angle redirection (b) Scaling up

Figure 18: One-way ANOVA test results.

scale distortions (1.66x and 1.67x for barefoot and shod conditions, respectively). Considering that we only count the answer with high confidence in the answer, this model does not accurately reflect the nuances of the study. Moreover, due to the highly constrained guess and lapse rate, it does not take into account the participant behavior properly, resulting in simplified model. This is reflected in more conservative threshold estimates

Fourth, though the DTs for shod conditions were consistently higher than those for barefoot conditions across all models, the ANOVA test showed that the difference between the intercept and slope parameters for both conditions do not have significant difference. So it is not enough to conclude that footwear has an effect on the perception. The same conclusion was drawn in the original paper via Wilcoxon signed-rank test.

6 Conclusion

These results emphasize the importance of selecting appropriate models for analyzing psychometric data in VR research. Accounting for the participant behavior, their randomness, guessing and lapsing pattern can significantly calibrate the detection thresholds by making user-specific and comprehensive system modifications. Future work may include the exploration of different sigmoid-shape functions such as cumulative normal distribution and more comprehensive look into the impact of footwear condition.

References

[1] Parastoo Abtahi and Sean Follmer. “Visuo-Haptic Illusions for Improving the Perceived Performance of Shape Displays”. In: *Proceedings of the 2018 CHI Conference on Human Factors in Computing Systems*. CHI ’18. Montreal QC, Canada: Association for Computing Machinery, 2018, pp. 1–13. ISBN: 9781450356206. DOI: 10.1145/3173574.3173724. URL: https://doi.org/10.1145/3173574.3173724.

[2] Nargiz Askarbekkyzy. "Designing visuo-haptic illusions for Virtual Reality applications using floor-based shape-changing displays". In: *IASDR 2023: Life-Changing Design*. IASDR 2023. Design Research Society, Oct. 2023. DOI: 10.21606/iasdr.2023.466. URL: http://dx.doi.org/10.21606/iasdr.2023.466.

[3] Yuki Ban et al. "Modifying an identified curved surface shape using pseudo-haptic effect". In: *2012 IEEE Haptics Symposium (HAPTICS)*. 2012, pp. 211–216. DOI: 10.1109/HAPTIC.2012.6183793.

[4] Kim Laranang Hansen et al. "FeetBack: Providing Haptic Directional Cues Through a Shape-changing Floor". In: *Nordic Human-Computer Interaction Conference*. NordiCHI '22. Aarhus, Denmark: Association for Computing Machinery, 2022. ISBN: 9781450396998. DOI: 10.1145/3546155.3546653. URL: https://doi.org/10.1145/3546155.3546653.

[5] Seungwoo Je et al. "Elevate: A Walkable Pin-Array for Large Shape-Changing Terrains". In: *Proceedings of the 2021 CHI Conference on Human Factors in Computing Systems*. CHI '21. Yokohama, Japan: Association for Computing Machinery, 2021. ISBN: 9781450380966. DOI: 10.1145/3411764.3445454. URL: https://doi.org/10.1145/3411764.3445454.

[6] Anatole Lécuyer. "Simulating Haptic Feedback Using Vision: A Survey of Research and Applications of Pseudo-Haptic Feedback". In: *Presence: Teleoperators and Virtual Environments* 18.1 (Feb. 2009), pp. 39–53. DOI: 10.1162/pres.18.1.39. eprint: https://direct.mit.edu/pvar/article-pdf/18/1/39/1624884/pres.18.1.39.pdf. URL: https://doi.org/10.1162/pres.18.1.39.

[7] Maud Marchal et al. "Multimodal Rendering of Walking Over Virtual Grounds". In: *Human Walking in Virtual Environments: Perception, Technology, and Applications*. Ed. by Frank Steinicke et al. New York, NY: Springer New York, 2013, pp. 263–295. ISBN: 978-1-4419-8432-6. DOI: 10.1007/978-1-4419-8432-6_12. URL: https://doi.org/10.1007/978-1-4419-8432-6_12.

[8] Shogo Okamoto et al. "Spectrum-based synthesis of vibrotactile stimuli: active footstep display for crinkle of fragile structures". In: *Virtual Reality* 17.3 (Mar. 2013), pp. 181–191. ISSN: 1434-9957. DOI: 10.1007/s10055-013-0224-y. URL: http://dx.doi.org/10.1007/s10055-013-0224-y.

[9] Gonçalo Padrao et al. "Violating body movement semantics: Neural signatures of self-generated and external-generated errors". In: *NeuroImage* 124 (2016), pp. 147–156. ISSN: 1053-8119. DOI: https://doi.org/10.1016/j.neuroimage.2015.08.022. URL: https://www.sciencedirect.com/science/article/pii/S1053811915007314.

[10] Irvin Rock and Jack Victor. "Vision and Touch: An Experimentally Created Conflict between the Two Senses". In: *Science* 143.3606 (1964), pp. 594–596. DOI: 10.1126/science.143.3606.594. eprint: https://www.science.org/doi/pdf/10.1126/science.143.3606.594. URL: https://www.science.org/doi/abs/10.1126/science.143.3606.594.

[11] Ryo Suzuki et al. "LiftTiles: Constructive Building Blocks for Prototyping Room-scale Shape-changing Interfaces". In: *Proceedings of the Fourteenth International Conference on Tangible, Embedded, and Embodied Interaction*. TEI '20. Sydney NSW, Australia: Association for Computing Machinery, 2020, pp. 143–151. ISBN: 9781450361071. DOI: 10.1145/3374920.3374941. URL: https://doi.org/10.1145/3374920.3374941.

[12] Shan-Yuan Teng et al. "TilePoP: Tile-type Pop-up Prop for Virtual Reality". In: *Proceedings of the 32nd Annual ACM Symposium on User Interface Software and Technology*. UIST '19. New Orleans, LA, USA: Association for Computing Machinery, 2019, pp. 639–649. ISBN: 9781450368162. DOI: 10.1145/3332165.3347958. URL: https://doi.org/10.1145/3332165.3347958.

[13] Yon Visell, Alvin Law, and Jeremy R. Cooperstock. "Touch Is Everywhere: Floor Surfaces as Ambient Haptic Interfaces". In: *IEEE Transactions on Haptics* 2.3 (2009), pp. 148–159. DOI: 10.1109/TOH.2009.31.

[14] Felix A. Wichmann and N. Jeremy Hill. "The psychometric function: I. Fitting, sampling, and goodness of fit". In: *Perception amp; Psychophysics* 63.8 (Nov. 2001), pp. 1293–1313. ISSN: 1532-5962. DOI: 10.3758/bf03194544. URL: http://dx.doi.org/10.3758/BF03194544.